Available online at www.sciencedirect.com
ScienceDirect
Polymer 48 (2007) 3437–3443
polymer
www.elsevier.com/locate/polymer

Synthesis and pH-dependent micellization of 2-(diisopropylamino)ethyl methacrylate based amphiphilic diblock copolymers via RAFT polymerization

Ying Qian Hu [a], Min Sang Kim [b], Bong Sup Kim [a], Doo Sung Lee [b,*]

[a] Polymer Technology Institute, Sungkyunkwan University, Suwon, Gyeonggi 440-746, Republic of Korea
[b] Department of Polymer Science and Engineering, Sungkyunkwan University, Suwon, Gyeonggi 440-746, Republic of Korea

Received 20 February 2007; received in revised form 9 April 2007; accepted 11 April 2007
Available online 19 April 2007

Abstract

The polymerization of 2-(diisopropylamino)ethyl methacrylate (DPA) by RAFT mechanism in the presence of 4-cyanopentanoic acid dithiobenzoate in 1,4-dioxane was studied. The DPA homopolymer was employed as a macro chain transfer agent to synthesize pH-sensitive amphiphilic block copolymers using poly(ethylene glycol) methyl ether methacrylate (PEGMA) as the hydrophilic block. ^{1}H NMR and GPC measurements confirmed the successful synthesis of these copolymers. Potentiometric titrations and fluorescence experiments proved that the copolymers underwent a sharp transition from unimers to micelles at a pH of ~6.7 in phosphate buffered saline solutions. It was found that the hydrophilic/hydrophobic balance of these block copolymers had no apparent effect on their pH-induced micellization behaviors. The DLS investigation revealed that the micelles have a mean hydrodynamic diameter below 60 nm with a narrow size distribution.
© 2007 Elsevier Ltd. All rights reserved.

Keywords: Amphiphilic diblock copolymer; pH-sensitive micelles; Reversible addition–fragmentation chain transfer (RAFT) polymerization

1. Introduction

Over the past decade, amphiphilic block copolymers have received much attention in many fields, due to their fascinating property of self-assembling into core–shell structured polymeric micelles in selective solvents, which have various potential applications [1–5]. Regarding the drug delivery application, such nanosized micelles are of particular importance by providing the advantages of efficient stabilization and delivery of poorly water-soluble, hydrophobic, and/or highly toxic anticancer drugs, with the ability to escape from the capture of reticuloendothelial systems (RES) and accumulate preferentially in solid tumor tissue through the enhanced permeability and retention (EPR) effect [6]. Furthermore, considering the lower extracellular pH value of the tumor cells than that of the normal tissue, site-specific release of therapeutic agents could be achieved by the utilization of pH-sensitive micelles [7,8]. These intelligent systems are usually stable under physiological pH conditions and could be triggered to release their contents upon exposure to decreased pH at the tumor site [9].

It was reported that 2-(diisopropylamino)ethyl methacrylate (DPA) homopolymer could be a promising pH-sensitive moiety with a pK_b of around 6.2, which was soluble in acidic solution as a cationic polyelectrolyte by protonation of its amine groups but became highly hydrophobic at around neutral pH [10,11]. Armes and co-workers [12] synthesized well-defined diblock copolymers of 2-methacryloyloxyethyl phosphorylcholine (MPC) and DPA by atom transfer radical polymerization (ATRP) and found that these materials were biocompatible with negligible cytotoxicities.

Recent development of reversible addition–fragmentation chain transfer (RAFT) polymerization offered a powerful synthetic tool for implementing the precise control of the polymer

* Corresponding author. Tel.: +82 31 290 7282; fax: +82 31 292 8790.
E-mail address: dslee@skku.edu (D.S. Lee).

0032-3861/$ - see front matter © 2007 Elsevier Ltd. All rights reserved.
doi:10.1016/j.polymer.2007.04.011

architecture and molecular weight (MW) as well as its distribution [13–18]. Compared with ATRP, RAFT is a metal-free process and therefore could avoid the contamination of the product by transition metal catalyst, which is vitally important for biomedical applications. However, to the best of our knowledge, there is no published reference available concerning the RAFT polymerization of DPA. In addition, the influence of the hydrophilic/hydrophobic balance on the pH-responsivity of this type of copolymers was also not reported systematically. The lack of such data drove us to investigate the homopolymerization and block copolymerization of DPA via RAFT.

In this study, DPA was polymerized by RAFT using 4-cyanopentanoic acid dithiobenzoate as a chain transfer agent (CTA) in 1,4-dioxane, and the homopolymer was employed as a macro-CTA to synthesize diblock copolymers with hydrophilic poly(ethylene glycol) methyl ether methacrylate (PEGMA). The controllability of the polymerization and the pH-sensitive micellization of the obtained copolymers were studied in detail.

2. Experimental section

2.1. Materials

DPA (98%, Scientific Polymer Products) and PEGMA (M_n ~475, Aldrich) were purified by passing through a basic alumina column to remove the inhibitor. 2,2′-Azobis(isobutyronitrile) (AIBN) was obtained from Junsei Co. (Tokyo) and recrystallized from methanol twice prior to use. Anhydrous 1,4-dioxane (99.8%) and all the other reagents were obtained from Aldrich and used as received. 4-Cyanopentanoic acid dithiobenzoate was synthesized according to a previously described procedure [19]. ^{1}H NMR (500 MHz, $CDCl_3$) δ: 1.97 (s, 3H, CH_3), 2.46–2.78 (m, 4H, C–CH_2–CH_2–C=O), 7.41 (m, 2H, H3 in phenyl), 7.59 (m, 1H, H4 in phenyl), 7.92 (m, 2H, H2 in phenyl).

2.2. Homopolymerization of DPA by RAFT

The homopolymerization of DPA was performed at a fixed CTA concentration of 0.03 M in 1,4-dioxane using AIBN as an initiator. The ratios of DPA/CTA and CTA/AIBN were varied to assess the control of the conversion and molecular weight by RAFT mechanism. Aliquots (10 mL) of the stock solution comprising CTA, AIBN, DPA and 1,4-dioxane were transferred to individual 50-mL Schlenk tubes and sealed with rubber septa. Each tube was degassed with nitrogen for 30 min and then immersed in a 70 °C oil bath. The polymerization was conducted under stirring for a predetermined time and then stopped by cooling in −40 °C acetone. The resulting mixture was analyzed directly by ^{1}H NMR spectroscopy in $CDCl_3$ to determine the monomer conversion.

For the preparation of DPA homopolymer-based macro-CTA for the subsequent block copolymerization, CTA (0.1675 g, 0.6 mmol), AIBN (0.0197 g, 0.12 mmol), DPA (6.42 g, 30 mmol) and 1,4-dioxane (20 mL) were introduced into a 100-mL Schlenk tube. After being bubbled with nitrogen for 30 min, the tube was sealed and heated at 70 °C with stirring for 5 h. The polymerization was terminated by quenching in liquid nitrogen. The resulting solution was concentrated and the product was precipitated into methanol, and then dried in vacuum.

2.3. RAFT polymerization of the block copolymers

Typically, DPA macro-CTA (0.69 g, 0.1 mmol, PDI = 1.19), AIBN (0.0028 g, 0.0167 mmol) and PEGMA (4.75 g, 10 mmol) were dissolved in 1,4-dioxane (20 mL), and the solution was purged with nitrogen for 30 min. Polymerization was carried out at 70 °C for 6 h. The resulting mixture was dialyzed (MWCO 3500) against water and then freeze-dried to give the final product. The method to investigate the monomer conversion was similar to that described above.

2.4. Measurements

^{1}H NMR spectra were recorded on a Unity Inova 500NB spectrometer (Varian, USA) using $CDCl_3$ as solvent and tetramethylsilane (TMS) as the internal reference. The molecular weight and its distribution were determined by gel permeation chromatography (GPC) at 45 °C with two columns (KF-802.5, KF-803L, Shodex, Japan) and a refractive index (RI) detector (Shodex RI-101), using tetrahydrofuran (THF) as the eluent at a flow rate of 0.8 mL/min. Narrowly distributed PMMAs (Shodex) were employed as standards.

The base dissociation constant (pK_b) values of the polymers were measured by potentiometric titrations with a Denver UB-10 pH meter (Denver Instrument, USA). First, 40 mL of 1–3 mg/mL polymer solution was adjusted to pH 3 with 1 M HCl solution. Then, titration curves were obtained by monitoring the pH increases of the solution with the addition of 0.1 M NaOH solution in increments of 0.05 mL. The pK_b value was defined as the midpoint of the plateau in the titration curve.

The pH sensitivity and critical micelle concentration (CMC) of the copolymers were estimated by fluorescence spectroscopy using pyrene as a probe. Fluorescence spectra were recorded by an Aminco-Bowman Series 2 luminescence spectrometer (SLM-Aminco, USA) at room temperature. Polymer solutions (1 mg/mL in phosphate buffered saline (PBS) solution) containing pyrene were prepared with different pH values and equilibrated for 6 h to assess the pH-induced micellization. The CMC was determined using polymer/pyrene solution at pH 7.4 with various concentrations. The final concentration of pyrene in all solutions was 6.0×10^{-7} M. The excitation spectra were recorded from 310 to 350 nm with an emission wavelength of 392 nm. The intensity ratios of I_{337}/I_{334} were used to evaluate the micelle formation.

The intensity-average hydrodynamic diameters of the micelles were measured by dynamic light scattering (DLS) on a Malvern PCS100 instrument equipped with a Brookhaven BI-9000AT digital correlator and a He–Ne laser at 633 nm. The concentration of all samples in PBS was 2–3 mg/mL.

The solution was filtered through a 1.2 μm filter. Measurements were performed at 25 °C with a scattering angle of 90°.

3. Results and discussion

3.1. Homo and block copolymerization

RAFT polymerization has proved more versatile with respect to the tolerance for the functional groups of monomers than other living/controlled free radical polymerization techniques. It could be applied to the controlled polymerization of a wide range of monomers under mild conditions, yielding polymers with predetermined molecular weights, low polydispersity indices (PDI) and advanced architecture. In this study, for the investigation of the polymerization kinetics of DPA, two sets of homopolymerization were conducted with different target degrees of polymerization (DP = 50 or 80) while keeping the other conditions constant. In Fig. 1(a) (target DP = 80), the time–conversion relationship and the pseudo-first-order kinetic plot are quite consistent with the features of living polymerization, indicating a rapid attainment of the main equilibrium and a constant number of radical propagating chains. There seemed no retardation occurring in these systems and the polymerization proceeded smoothly with a higher monomer conversion of 75% after 6 h. In Fig. 1(b), the livingness of this system was further confirmed by the linear increase of MW with the conversion and the narrow polydispersity (below 1.18) throughout the polymerization. However, slight positive deviations from the theoretical MWs should be noted in the initial stage. The positive *y*-intercept might result from a higher polymerization rate than that of the addition of growing radicals to the CTA [20,21]. In spite of this, the PDI of the resultant polymers were still low, suggesting that the possible AIBN-derived chains had little effect on the RAFT process. The evolution of the GPC curves clearly showed a peak shift to higher MWs with increasing reaction time (Fig. 1(c)). All the GPC elution curves were unimodal and symmetrical in the first 4 h. However, after 4 h, some small tailings could be observed in the GPC chromatograms, which should be yielded from irreversible termination reactions. Meanwhile, the corresponding PDI slightly increased. In the case of the polymerization with a target DP of 50, similar results exhibiting good controllability were obtained (data not shown).

As expected, the polymerization rate increased with the decreasing CTA/AIBN ratio from 10/1 to 3/1 (Table 1). Even at a high CTA/AIBN ratio of 3/1, the polymerization still exhibited a controlled character (PDI < 1.21). The DPA macro-CTAs with different chain lengths were obtained by adjusting the monomer/CTA ratio as well as the reaction time according to the kinetic results. Fig. 2 shows a typical ^{1}H NMR spectrum of DPA homopolymer, in which the peaks located at 2.64, 3.00, and 3.84 ppm correspond to the resonance of $-NCH_2-$, $-NCH-$, and $-COOCH_2-$ in the side chains, respectively. In the ^{1}H NMR spectra, the resonance signals of the aromatic protons appear at around 7.4–7.9 ppm, indicating that most of the CTA moiety remained at one end of the polymer.

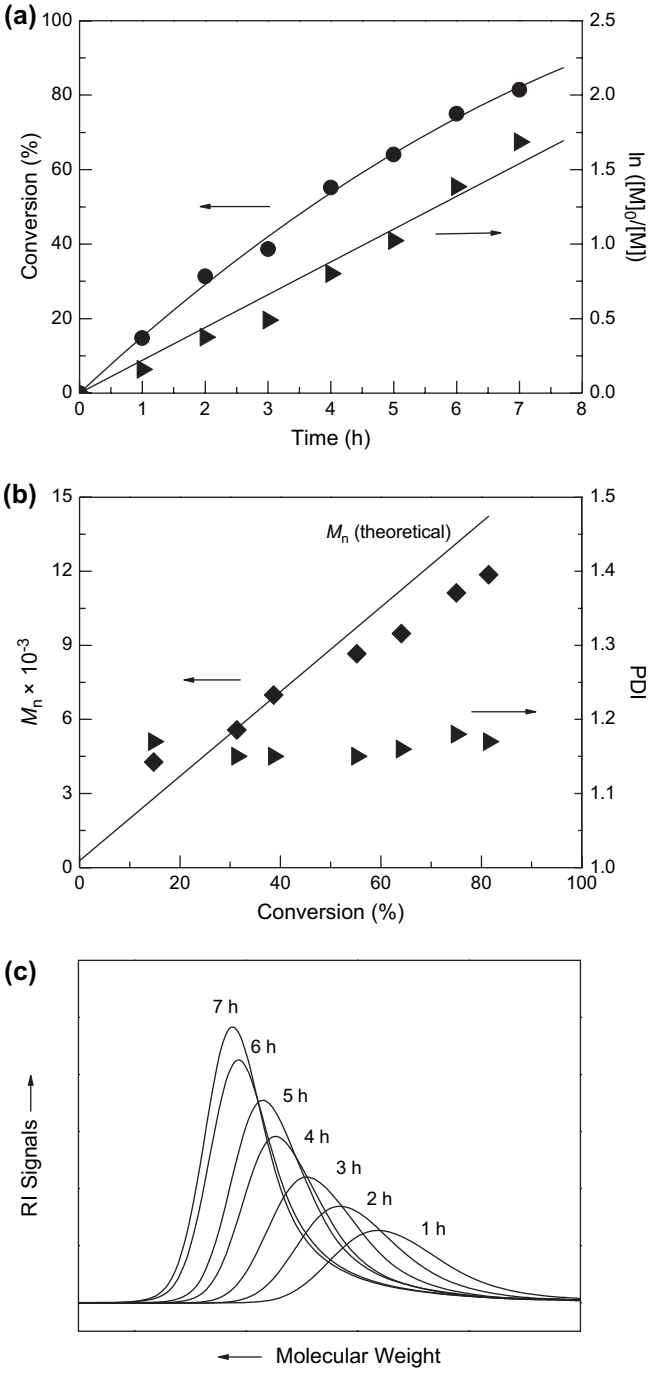

Fig. 1. Homopolymerization of DPA ($[M]_0/[CTA]_0/[AIBN]_0 = 80:1:0.2$, $[CTA]_0 = 0.03$ M): conversion and ln ($[M]_0/[M]$) versus polymerization time (a), M_n and PDI versus conversion (b), and evolution of GPC curves (c) with the reaction time.

For preparing amphiphilic DPA–PEGMA diblock copolymers, the polymerization of PEGMA was carried out by RAFT process in the presence of the DPA macro-CTA. Likewise, a linear increase was observed in the pseudo-first-order kinetic plot (Fig. 3), implying the controlled manner of the copolymerization. The polymerization showed a fast rate and a monomer conversion of 72% was reached after 6 h. The formation of the diblock copolymers was then confirmed by

Table 1
RAFT homopolymerization of DPA in 1,4-dioxane at 70 °C using 4-cyanopentanoic acid dithiobenzoate as the CTA ($[CTA]_0 = 0.03$ M)

Expt. no.	Target DP	$[CTA]_0/[AIBN]_0$	Time (h)	Conv.[a] (%)	$M_{n,th}$[b]	M_n[c] (GPC)	PDI[c]
h1	50	5/1	6	74.5	8250	7570	1.13
h2	50	3/1	2	43.4	4930	4700	1.17
h3	50	3/1	5	84.3	9300	8760	1.18
h4	80	5/1	6	75.0	13,120	11,130	1.18
h5	80	3/1	5	79.3	13,860	12,150	1.21
h6	80	10/1	6	64.1	11,250	9480	1.16
h7	100	5/1	6	65.1	14,210	12,690	1.21

[a] Determined by ^{1}H NMR in $CDCl_3$.
[b] Theoretical $M_n = [M]_0/[CTA]_0 \times \text{conv.} \times MW_{DPA} + MW_{CTA}$.
[c] Determined by GPC in THF using PMMA as standards.

GPC. A significant shift toward higher MWs could be observed in the GPC chromatograms with no obvious coexistence of PEGMA homopolymer, which confirmed that the majority of the DPA macro-CTA was effectively living. However, some tailing can be detected, indicative of the existence of a small number of dead chains. Consequently, the PDI values of the resulting copolymers were relatively increased (around 1.4). On the other hand, the substantial difference in the hydrodynamic volumes between the copolymers and PMMA standards was also responsible for the higher PDI values and the obvious deviations of the experimental MWs from the corresponding theoretical ones (Table 2).

Fig. 4 shows a typical ^{1}H NMR spectrum for the block copolymer. The molar ratios of these two blocks were calculated from the ^{1}H NMR spectra using the relative intensities between the −NC*H*− signal in DPA (3.00 ppm) and the C*H*$_3$− in the PEGMA side chains (3.39 ppm). A series of block copolymers with various PEGMA sequence lengths were prepared using the same DPA macro-CTA (DPA_{31}, where 31 is the number-average DP). The copolymers with different

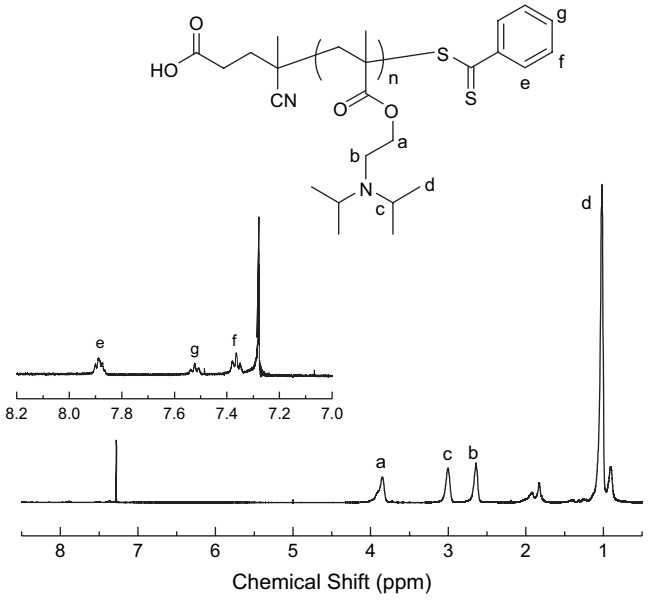

Fig. 2. ^{1}H NMR spectrum of DPA homopolymer in $CDCl_3$.

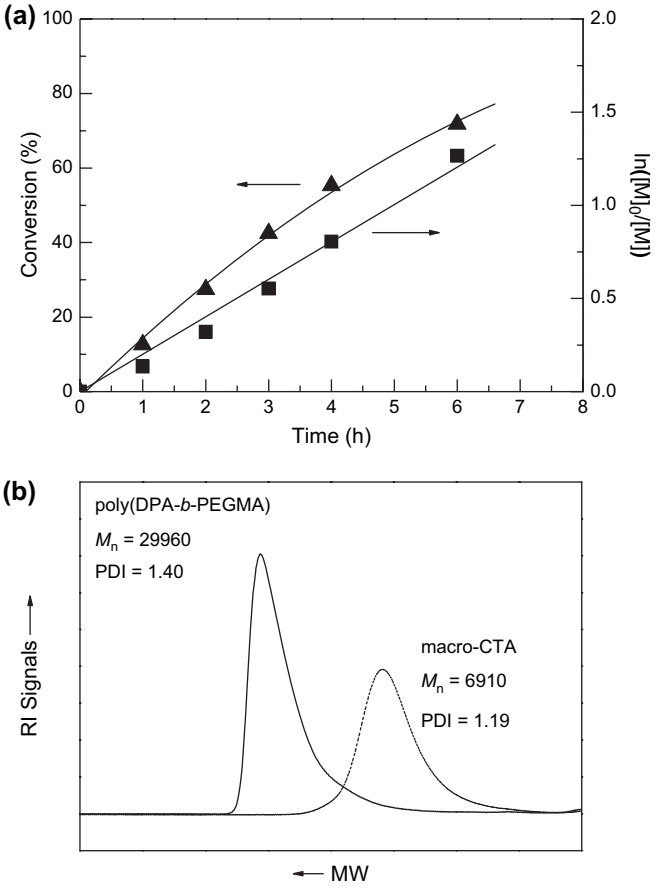

Fig. 3. Kinetics (a) and the GPC curves (b) of the block copolymerization of PEGMA using DPA homopolymer as the macro-CTA in 1,4-dioxane at 70 °C.

DPA block lengths and similar PEGMA block length were also obtained.

3.2. Potentiometric titration

The pK_b value is a critical parameter of the pH-sensitive polymers, especially for drug delivery, which has a decisive influence on the phase transition of the micelle. However, the relevant reports on the pK_b of DPA-based polymers in the literature generally give a simple and puzzling result (ranging from 5.6 to 6.2, depending on the copolymer composition) [11,22]. It is very important to clarify how the polymer

Table 2
Block copolymerization of DPA with PEGMA using PDPA as the macro-CTA ($[CTA]_0 = 0.005$ M, $[PEGMA]_0/[CTA]_0/[AIBN]_0 = 600:6:1$)

Sample	DP of PDPA	Time (h)	Conv.[a] (%)	$M_{n,th}$[b]	M_n[c] (GPC)	PDI[c]
DPA_{31}−$PEGMA_{29}$	31	2	30.6	21,450	18,640	1.42
DPA_{31}−$PEGMA_{62}$	31	4	61.7	36,220	25,820	1.42
DPA_{31}−$PEGMA_{74}$	31	6	74.2	42,160	29,960	1.40
DPA_{44}−$PEGMA_{79}$	44	6	78.8	44,350	31,750	1.46
DPA_{65}−$PEGMA_{71}$	65	5	71.2	48,010	36,830	1.44

[a] Determined by ^{1}H NMR in $CDCl_3$.
[b] Theoretical $M_n = [M]_0/[CTA]_0 \times \text{conv.} \times MW_{PEGMA} + MW_{macro\text{-}CTA}$.
[c] Determined by GPC in THF using PMMA as standards.

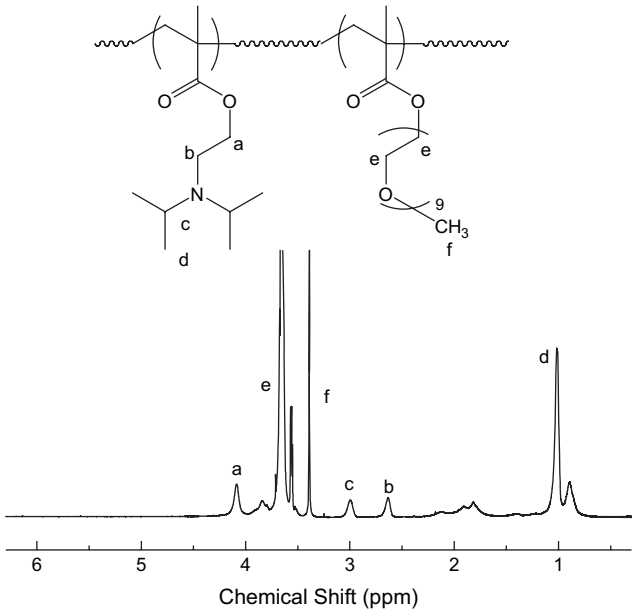

Fig. 4. A typical ^{1}H NMR spectrum of DPA-*b*-PEGMA diblock copolymer in $CDCl_3$.

composition influences the pK_b values of these materials for bio-related applications. The typical potentiometric titration profiles are shown in Fig. 5. The (co)polymers were first dissolved in acidic solution by the protonation of the tertiary amine groups. As NaOH was gradually added, the solution pH increased until a plateau was reached, corresponding to the deprotonation process of the ionized amine residues, in which the hydrophilicity of the DPA block was progressively decreased. When the pH was above a critical value, the DPA blocks became hydrophobic and trended insoluble. The pK_b values of around 6.04 could be obtained for the DPA_{31} and DPA_{44} homopolymer in pure water. However, a slightly lower pK_b of 5.89 was detected for the DPA_{65} homopolymer. This phenomenon might result from the increased steric hindrance and thus the reduced accessibility of amine groups by hydrogen ions with the MW increase. As for the block copolymers, it was found that the pK_b values shifted to slightly higher values, which might be due to the notable hydration of the PEGMA blocks [23]. The pK_b values were found to be around 6.17 for the copolymers DPA_{31}–$PEGMA_n$ ($n = 29$, 62, or 74) and DPA_{44}–$PEGMA_{79}$.

It was reported that ionic strength could lead to the conformation changes of polyelectrolyte chains in aqueous solution [24]. For this reason, NaCl was added to the polymer solution with a final concentration of 0.15 M to mimic the ionic strength in human body. The subsequent results for all the samples showed a noticeable rise in the pK_b values with an almost same increment. This phenomenon was consistent with the findings for weak polyelectrolytes in the literature and could be explained as follows. The addition of NaCl caused the shielding of the charges along the DPA chains, thus stabilizing the protonated structures. As a result, the equilibrium between the protonated and deprotonated amine groups shifted toward the formation of the former structure and the critical

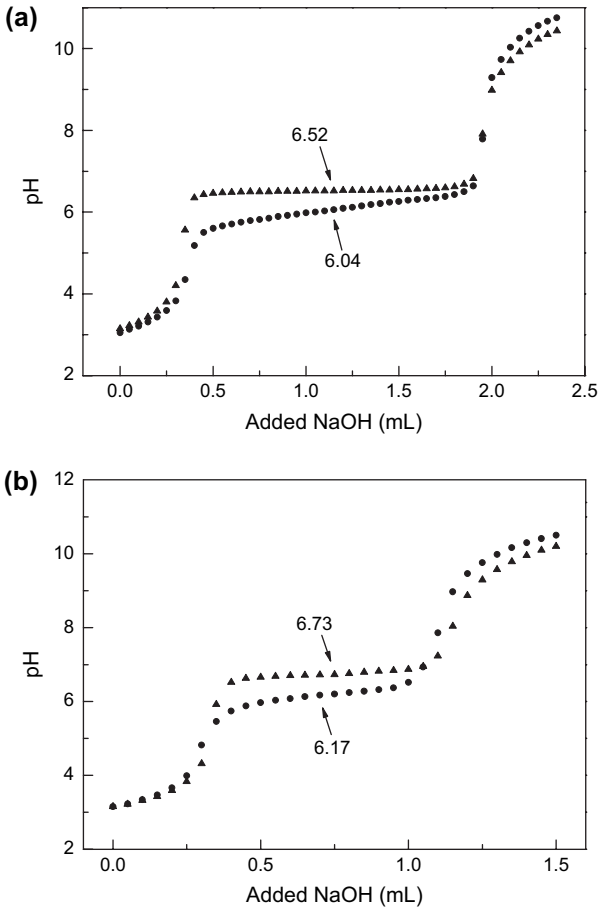

Fig. 5. Potentiometric titration curves of DPA homopolymer (a), and DPA_{31}–$PEGMA_{62}$ block copolymer (b) at different ionic strengths (●: ~0; ▲: 0.15 M).

transition pH thus increased [25]. At an ionic strength of 0.15 M, the pK_b values increased to 6.52 for the DPA_{31} homopolymer, around 6.73 for DPA_{31}–$PEGMA_n$ ($n = 29$, 62, or 74) copolymers, 6.65 for DPA_{44}–$PEGMA_{79}$, and 6.57 for DPA_{65}–$PEGMA_{71}$ copolymer, respectively. That is to say, for a given DPA block length, the pK_b values of the copolymers hardly changed with the variation of the hydrophilic block lengths. In addition, there was no apparent dependence of the pK_b on the DP of these polymers. This result was similar to that for the case of polystyrene-based cationic block copolymers using *N*,*N*-dimethylvinylbenzylamine as a pH-sensitive moiety [26], in which the pK_b decreased from 7.3 to 7.1 as the length of the core block increased from 11 to 22, but the decrease became much less pronounced as the DP further increased.

3.3. Micellization behavior

The pH-induced micellization was detected by fluorescence spectroscopy in PBS solution. Pyrene was used as a probe due to its high sensitivity to the surrounding polarity. With the increase of the solution pH, the positively charged DPA units were progressively deprotonated and hence became hydrophobic and shrunk. When the critical micellization pH (pH*) was

reached, the hydrophobic DPA chains aggregated into coils and thereby formed hydrophobic microdomains. As shown in Fig. 6(a), the sharp increase of I_{337}/I_{334} at pH ~6.7 corresponds to the significant change of the surrounding polarity encountered by pyrene. However, there seemed no obvious variation in the pH* values among the copolymers with different compositions, except for a somewhat lower value (~6.5) of DPA_{65}–$PEGMA_{71}$ copolymer. That is to say, the hydrophilic/hydrophobic balance of these block copolymers had little effect on their pH-induced micellization behaviors, which was consistent with the results of potentiometric titration.

In general, the pK_b, at which half of the ionizable groups are ionized, is much related to pH*. However, they are not exactly matched in some cases because the conformational transition of the polymer chains, which occurs at pH*, is governed by the balance between the electrostatic repulsions and hydrophobic interactions. It was established that the introduction of hydrophobic moiety could regulate the pH*, but the pK_b could be only slightly influenced [9]. In this study, DPA has larger hydrophobic groups at the pendent amine atoms and thus has stronger hydrophobic interactions above its pK_b, which can cause a stable hydrophobic microenvironment for the pyrene probe with lower MW. As a result, the pyrene probe entrapped in the formed compact micellar core is not sensitive to the MW change of either the hydrophobic or hydrophilic blocks. Conversely, for the polymers with weaker hydrophobic interactions, the surrounding polarity of pyrene varies with the change of the MW and thereby the pH* depends on the polymer chain length, as observed for PEG–poly(β-amino ester) (PAE) block copolymers reported by our group [8], in which the relative lengths of the hydrophilic and ionizable blocks were important factors for pH sensitivity.

CMC is also an important parameter of polymeric micelles for drug delivery, related to the micelle stability in the blood stream and even the drug release behavior. The CMC values for the DPA_{31}–$PEGMA_{29}$ and DPA_{31}–$PEGMA_{62}$ were 0.0026 and 0.0058 mg/mL, respectively. The low CMC values of these polymers could make the micelles thermodynamically stable after intravenous administration.

The variation in hydrodynamic diameters (D_h) as a function of the solution pH is shown in Fig. 7(a). At lower pHs, all the polymers were molecularly dissolved in the PBS solution and therefore no micelle could be detected by DLS. As the pH was

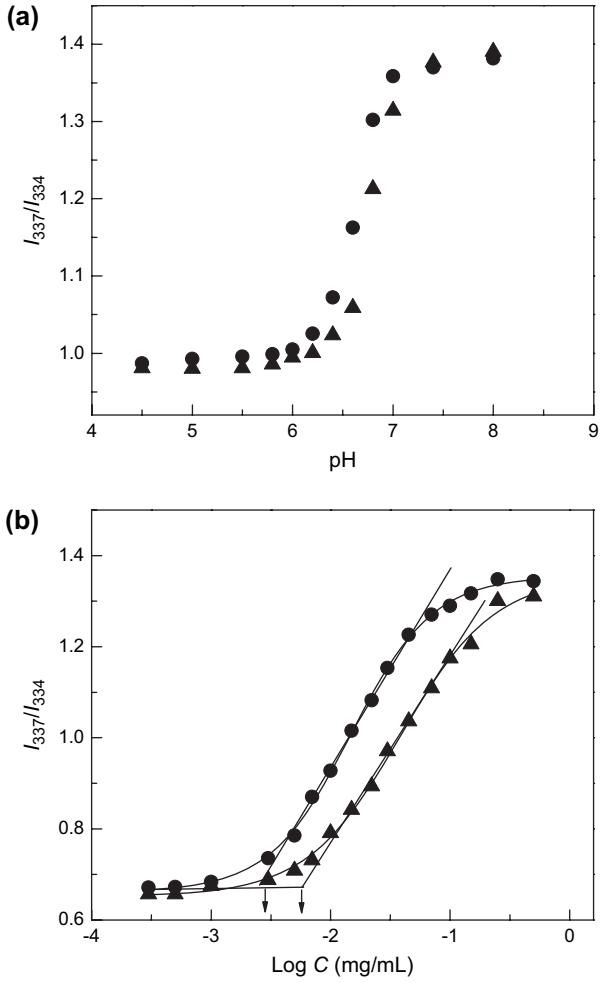

Fig. 6. I_{337}/I_{334} intensity ratios obtained from pyrene excitation spectra for DPA_{31}–$PEGMA_{29}$ (●), and DPA_{31}–$PEGMA_{62}$ (▲) in PBS solutions as a function of pH (a) and polymer concentration (b).

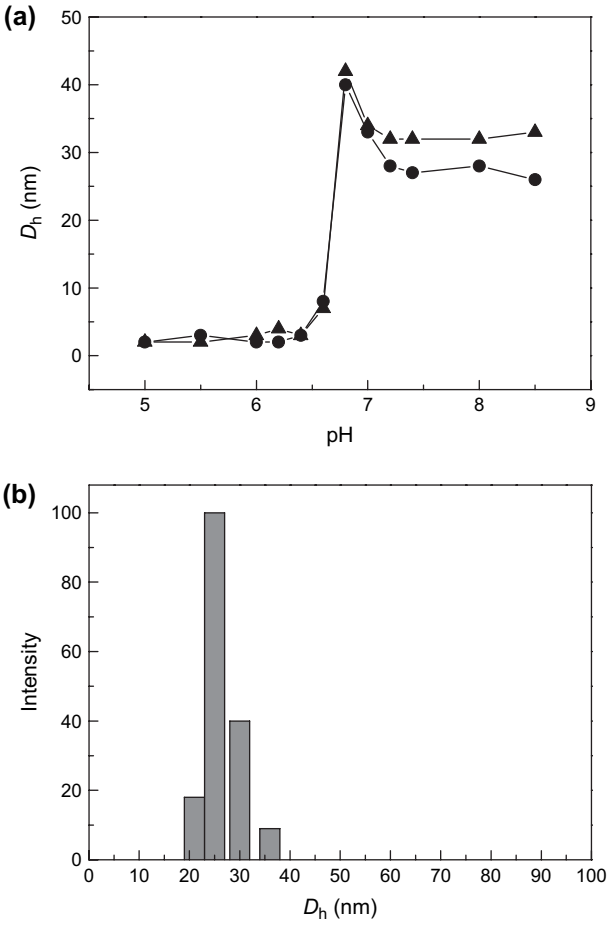

Fig. 7. DLS measurements: (a) average hydrodynamic diameters of the copolymers (●) DPA_{31}–$PEGMA_{29}$ and (▲) DPA_{31}–$PEGMA_{62}$ as a function of pH in PBS solutions, and (b) the size distribution of DPA_{31}–$PEGMA_{62}$.

increased, the hydrophobic interaction became predominant in the competition with the electrostatic repulsion in the DPA blocks. The formation of micelles occurred at around pH 6.6–6.8, which was consistent with the results obtained by fluorescence spectroscopy. However, this observation was different from the report by Bütün et al. [22], in which they simply described that as the DPA content of the 2-(dimethylamino)ethyl methacrylate (DMA)–DPA diblock copolymer was increased, micellization occurred at lower pH.

At pH 7.4, the average hydrodynamic diameters for the DPA_{31}–$PEGMA_{29}$, DPA_{31}–$PEGMA_{62}$, DPA_{31}–$PEGMA_{74}$, DPA_{44}–$PEGMA_{79}$ and DPA_{65}–$PEGMA_{71}$ copolymers were found to be 27, 32, 34, 36 and 59 nm, respectively. The noticeable D_h elevation of DPA_{65}–$PEGMA_{71}$ micelle could be attributed to the increase of the aggregation number with the increasing core block length. As can be seen, there was a decreasing tendency for the micelle size with the solution pH increasing from 6.8 to 7.2. This should be due to the incomplete deprotonation of the DPA blocks at pH 6.8 [27]. Consequently, the residual electrostatic repulsion among the charged amine groups hindered the dense packing of the DPA core, i.e., ill-defined micellar structures were formed at pH 6.8. Upon further pH increase to pH 7.2, the DPA blocks became completely deprotonated and micelles with denser cores were ultimately formed. It should be mentioned that the size distribution of the micelles maintained a narrow and near-monodisperse pattern for all samples, even at pH 6.8.

4. Conclusion

RAFT homopolymerization of DPA could proceed smoothly in a controlled manner using 4-cyanopentanoic acid dithiobenzoate as the CTA in 1,4-dioxane. Amphiphilic block copolymers of DPA and PEGMA were synthesized by employing DPA homopolymer as a macro-CTA. The copolymer showed a pH-induced self-assembly in PBS at pH $\sim$6.7. The hydrophilic/hydrophobic balance of these copolymers had no apparent effect on their pH-induced micellization behaviors. The DLS results showed that the mean size of the micelles was smaller than 60 nm with narrow and near-monodisperse size distributions. These pH-sensitive micelles might be useful for the targeted delivery of anticancer drugs.

Acknowledgements

This research was supported by the Korea Research Foundation ''KRF-2006-005-J04602''.

References

[1] Kataoka K, Harada A, Nagasaki Y. Adv Drug Deliv Rev 2001;47(1):113–31.
[2] Lukyanov AN, Torchilin VP. Adv Drug Deliv Rev 2004;56(10):1273–89.
[3] Yusa SI, Fukuda K, Yamamoto T, Ishihara K, Morishima Y. Biomacromolecules 2005;6(2):663–70.
[4] Zhang JX, Qiu LY, Zhu KJ, Jin Y. Macromol Rapid Commun 2004;25(19):1563–7.
[5] Liu B, Perrier S. J Polym Sci Part A Polym Chem 2005;43(16):3643–54.
[6] Haag R. Angew Chem Int Ed 2004;43(3):278–82.
[7] Lee ES, Na K, Bae YH. Nano Lett 2005;5(2):325–9.
[8] Kim MS, Hwang SJ, Han JK, Choi EK, Park HJ, Kim JS, et al. Macromol Rapid Commun 2006;27(6):447–51.
[9] Gil ES, Hudson SM. Prog Polym Sci 2004;29(12):1173–222.
[10] Ma YH, Tang Y, Billingham NC, Armes SP, Lewis AL, Lloyd AW, et al. Macromolecules 2003;36(10):3475–84.
[11] Licciardi M, Tang Y, Billingham NC, Armes SP, Lewis AL. Biomacromolecules 2005;6(2):1085–96.
[12] Salvage JP, Rose SF, Phillips GJ, Hanlon GW, Lloyd AW, Ma IY, et al. J Controlled Release 2005;104(2):259–70.
[13] Moad G, Rizzardo E, Thang SH. Aust J Chem 2005;58(6):379–410.
[14] Favier A, Charreyre MT. Macromol Rapid Commun 2006;27(9):653–92.
[15] Zhang LW, Chen YM. Polymer 2006;47(15):5259–66.
[16] You YZ, Oupický D. Biomacromolecules 2007;8(1):98–105.
[17] Lin Y, Liu XH, Li XR, Zhan J, Li YS. J Polym Sci Part A Polym Chem 2007;45(1):26–40.
[18] Fournier D, Hoogenboom R, Thijs HML, Paulus RM, Schubert US. Macromolecules 2007;40(4):915–20.
[19] Mitsukami Y, Donovan MS, Lowe AB, McCormick CL. Macromolecules 2001;34(7):2248–56.
[20] Vasilieva YA, Thomas DB, Scales CW, McCormick CL. Macromolecules 2004;37(8):2728–37.
[21] Garnier S, Laschewsky A. Macromolecules 2005;38(18):7580–92.
[22] Bütün V, Armes SP, Billingham NC. Polymer 2001;42(14):5993–6008.
[23] Lee ES, Shin HJ, Na K, Bae YH. J Controlled Release 2003;90(3):363–74.
[24] Lee AS, Gast AP, Butun V, Armes SP. Macromolecules 1999;32(13):4302–10.
[25] Giacomelli C, Men LL, Borsali R, Lai-Kee-Him J, Brisson A, Armes SP, et al. Biomacromolecules 2006;7(3):817–28.
[26] Mitsukami Y, Hashidzume A, Yusa SI, Morishima Y, Lowe AB, McCormick CL. Polymer 2006;47(12):4333–40.
[27] Zhu ZY, Armes SP, Liu SY. Macromolecules 2005;38(23):9803–12.